Nanostructures

DOI: 10.1002/anie.200701771

Form Emerges from Formless Entities: Temperature-Induced Self-Assembly and Growth of ZnO Nanoparticles into Zeptoliter Bowls and Troughs**

*Katla Sai Krishna, Uzma Mansoori, Naduvilethadathil Rajan Selvi, and Muthusamy Eswaramoorthy**

Construction of complex morphologies by controlled growth and organization of nanoparticles at multiple-length scales is one of the challenging tasks in materials synthesis.[1,2] Inorganic nano- and microstructures of prevalent shapes like rods, tubes, and spheres can be readily built from colloidal and ligand-stabilized nanoparticles[3–5] through self-assembly processes. However, engineering complex forms to parallel naturally existing biominerals is not a simple task and demands many new synthetic approaches.[6–8] Herein, we report for the first time a temperature-induced self-assembly and growth of ZnO nanoparticles into unusual bowl-, trough-, and ring-shaped structures. ZnO, an important wide-band-gap semiconductor, finds applications in catalysis,[9] solar cells,[10] sensors,[11] UV lasing,[12] and photoelectronics.[13] The properties of ZnO are closely related to its microstructures, particularly its crystal size, orientation, and morphology.[14] Though a variety of ZnO nano- and microstructures of various shapes have been obtained by solid–vapor phase growth (SVG),[15–21] microemulsion,[22] and hydrothermal methods,[23] bowl and triangular trough-shaped structures, to the best of our knowledge, have not been reported so far. We also demonstrate herein that the ZnO bowls and rings thus obtained can be used as a template to make metal or metal oxide replicas. The tiny bowls (of zeptoliter volume) are envisaged not only to hold fluids of ultralow volume,[24] but also to be used to grow nanoparticles,[25] immobilize biomolecules,[26] and screen sub-micrometer-sized particles.[27]

The field-emission scanning electron microscopy (FESEM) image of the ZnO bowls after calcining the composite (zinc nitrate/poly(vinyl pyrrolidone) (PVP) wt/wt ratio 0.5) at 600 °C for 5 h is shown in Figure 1 a. The bowls were obtained in good yield with the outer diameter varying from 300 nm to 1 μm. The background image shows a porous network made up of ZnO nanoparticles of size 30 to 80 nm. The bowls are not fully circular and in some cases they are faceted. The widths of the rims are in the range of 80 to 100 nm (Figure 1 b). The bowls have a coarse inner surface owing to variation in the sizes and shapes of the particles from which they are made.

The inner core of the bowl shown in Figure 1 b is composed of small particles, and its outer edge is formed by the fusion of large, elongated particles, which resembles the formation of microstructures of cocolith by the fusion of nanometer-scale calcite particles.[6] An atomic force microscopy (AFM) image and the height-profile analysis of a single bowl of size 300 nm show its depth to be around 90 nm. The

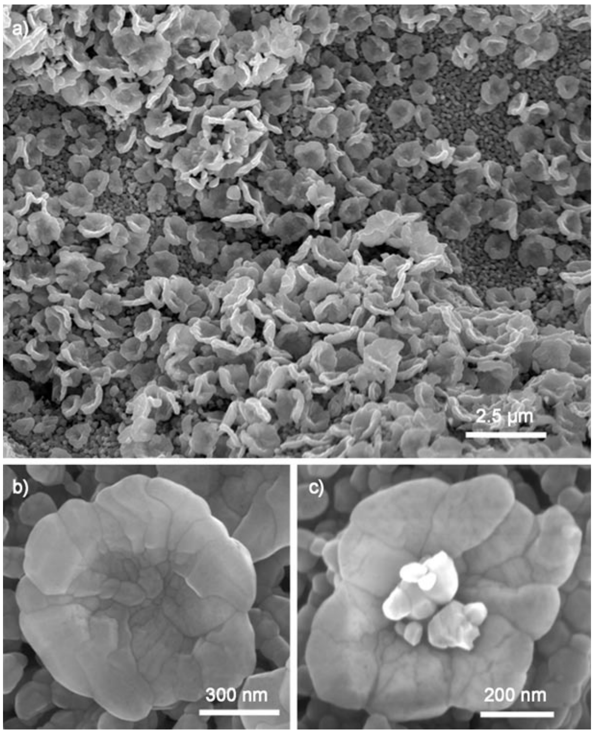

Figure 1. FESEM images of ZnO bowls formed at 600 °C. a) Low-magnification image showing high yield of sub-micrometer-sized ZnO bowls. b) High-magnification image of a single bowl. c) A ZnO bowl holding nanoparticles of ZnO.

---

[*] K. S. Krishna, N. R. Selvi, Dr. M. Eswaramoorthy
Chemistry and Physics of Materials Unit
and DST Unit on Nanoscience
Jawaharlal Nehru Centre for Advanced Scientific Research
Jakkur P.O., Bangalore 560064 (India)
Fax: (+91) 802-208-2766
E-mail: eswar@jncasr.ac.in
Homepage: http://www.jncasr.ac.in/eswar

U. Mansoori
Department of Chemistry
Aligarh Muslim University
Aligarh 202 002 (India)

[**] The authors thank Prof. C. N. R. Rao, FRS for the kind support and encouragement. U.M. thanks JNCASR for the Summer Research Fellowship. The authors acknowledge Chandramohan, Veeco-India Nanotechnology Laboratory for the AFM measurements.

Supporting information for this article is available on the WWW under http://www.angewandte.org or from the author.

volume calculated for a single bowl of size 300 nm is about 1 zeptoliter (see the Supporting Information, 1). An ultrasmall container fortuitously holding the ZnO nanoparticles of different sizes between 50 and 150 nm is shown in Figure 1c. Synthesis of ZnO using low-molecular-weight ($M_w = 40000$) PVP polymer also resulted in bowl-shaped structures in good yield. The magnified image of one bowl of approximate size 500 nm is again made up of nanoparticles of various sizes and shapes (see the Supporting Information, 2a). However, the yield of ZnO bowls is decreased when the PVP/zinc nitrate weight ratio is above 0.75 (see the Supporting Information, 2b).

To understand the role of PVP in the formation of ZnO bowls, we studied the morphology of ZnO–PVP composites calcined at different temperatures: 250, 370, 420, and 470 °C. These temperatures were selected on the basis of the decomposition temperatures of the precursors, zinc nitrate, and PVP, as obtained from thermogravimetric analysis (TGA; see the Supporting Information, 3). TGA shows that, at 370 °C, the zinc nitrate decomposes to ZnO, whereas the decomposition of PVP just begins. At 420 °C, the polymer is partially decomposed and, at 470 °C, it is decomposed completely. The powder X-ray diffraction (PXRD) pattern (see the Supporting Information, 4) confirms the formation of ZnO nanoparticles in the composite even at 250 °C. The peak broadening at lower calcination temperatures is associated with the formation of smaller nanoparticles. At higher calcination temperatures, the well-resolved peaks obtained can be indexed to the ZnO wurtzite phase. The size of the ZnO nanoparticles increases with an increase in calcination temperatures, which is reflected in the sharpening of the peak line width in the PXRD pattern.

FESEM images of the samples calcined at 370 °C show that ZnO nanoparticles of size around 10 to 30 nm are well-interspersed within the organic matrix (Figure 2a). Calcination at 420 °C for 5 h resulted in the formation of nanocomposite structures on the surface with bladelike morphologies of sizes between 100 and 400 nm (Figure 2b). A higher-magnification image (not shown) confirms the presence of an organic matrix studded with ZnO nanoparticles of sizes in the range 10 to 30 nm. Energy-dispersive X-ray analysis (EDX) of a bladelike nanostructure confirms the presence of carbon and nitrogen from the polymer matrix. Further growth and organization of these bladelike structures with concomitant removal of the polymer during calcination at 470 °C for 5 h resulted in the formation of mesoporous disks (Figure 2c). The enlarged image of a disk shown in the inset of Figure 2c indicates that the network of pores is made by the fusion of ZnO nanoparticles. The pore sizes in the disk are in the range 15 to 25 nm, and the thickness of the walls is about 20 nm. Extending the calcination time beyond 5 h at 470 °C up to 8 h modified these porous architectures into exotic morphologies such as bowls and triangular troughs (Figure 2d). The side-on view of a bowl shown in Figure 2e displays a rim thickness of about 100 nm. Prolonged heating (8 h) at the same temperature leaves no interconnected pores in these morphologies. However, the presence of many nanodents in the bowls is manifested from the lower electron-density contrast observed in the TEM image (see the Supporting Information, 5a). The electron diffraction pattern shows that the ZnO bowls are polycrystalline in nature (see the Supporting Information, 5b). A scanning transmission electron microscopy (STEM) image of a bowl with a nonporous surface shows many low-electron-density spots, suggesting the existence of nanocavities inside the walls of the bowls (see the Supporting Information, 5c,d). The Brauner–Emmett–Teller (BET) surface area for the samples calcined at 370 °C is well below 10 m^2 g, mostly owing to the nonporous nature of the ZnO–PVP composite film. Removal of polymer upon calcination at 470 °C for 5 h increases the surface area to about 40 m^2 g. The pore size analysis shows the appearances of additional

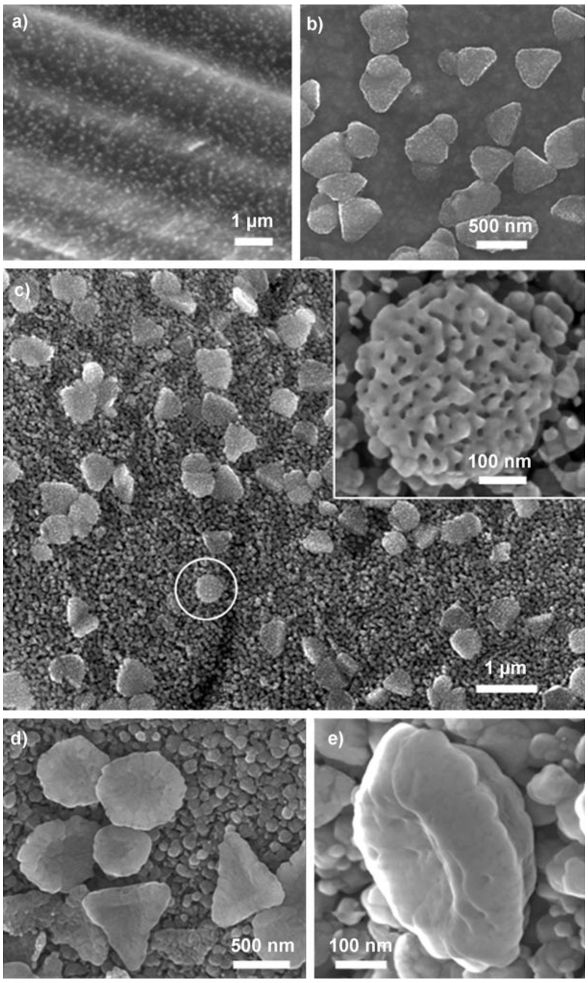

Figure 2. FESEM images showing intermediate morphologies at different calcination temperatures during bowl formation. a) At 370 °C (5 h), the precursor zinc nitrate in the composite film is completely decomposed into ZnO nanoparticles of approximate size 30 nm, which are well-dispersed within the partially decomposed polymer matrix. b) At 420 °C (5 h), a large number of ZnO–polymer nanocomposites of bladelike morphology in the size range 100 to 400 nm emerges from the surface. c) At 470 °C (5 h), aggregation of bladelike structures and concomitant removal of polymer results in nanoporous ZnO disks; inset: high-magnification image of the encircled portion shows a single mesoporous disk. The size of the nanopores are in the range 15 to 25 nm. d) At 470 °C for longer duration (8 h), ZnO bowls and triangular troughs are formed. e) Side-on view of a single ZnO bowl obtained at 470 °C with a rim thickness of 100 nm.

mesopores of size 15 to 25 nm (see the Supporting Information, 6), which is in accordance with the pore size observed in the FESEM image (Figure 2c). These larger pores, however, disappeared upon calcination of the samples at 600 °C, thus lending support to the transformation of mesoporous disks into sub-micrometer-sized bowls of ZnO. The corresponding BET surface area of the sample is around 28 m^2g.

We have also studied the effect of heating rate on the morphology by increasing the calcination temperature of the zinc nitrate–PVP composite to 600 °C at a heating rate of 20 °C min^{-1} and kept at that temperature for 1 h before it was cooled to room temperature. Interestingly, we observed the formation of ring-shaped ZnO nanostructures (Figure 3). These nanorings are corrugated in shape and each ring is made up of around 10 to 12 nanoparticles of approximate size 50 to 80 nm. The outer diameters of the rings are between 200 and 300 nm, with the inner hole between 50 and 100 nm. The intermediate morphologies obtained at different calcination temperatures and different time durations led us to believe that the bowls and triangular troughs emerge from the aggregation of two or three bladelike secondary structures (Figure 4a). Figure 4b gives a schematic of the formation of these microbowls.

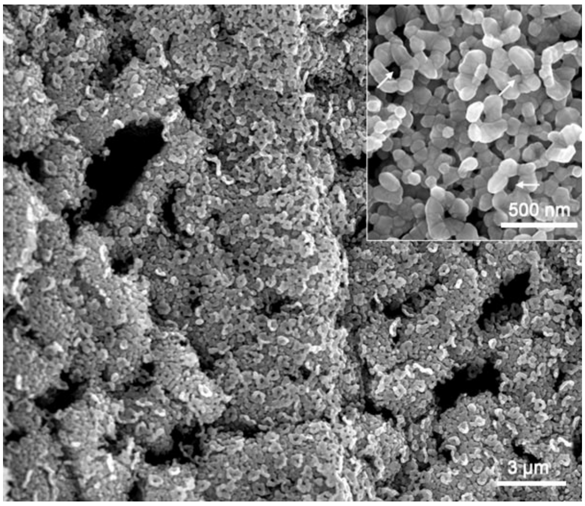

Figure 3. FESEM image of corrugated ring-shaped ZnO nanostructures: Calcination of the ZnO–PVP composite at 600 °C for 1 h duration with a faster rate of heating (20 °C min^{-1}) resulted in the formation of ZnO rings. Each of these rings is further made up of 10 to 12 ZnO nanoparticles of approximate sizes 50 to 80 nm; inset: magnified image of these rings with arrows pointing towards the holes.

In summary, we have succeeded in preparing zeptoliter bowls and troughs of ZnO by the temperature-induced self-assembly and growth of nanoparticles. These bowls could be used as a template to synthesize various metal and metal oxide bowls. To prove this point, we have made gold replicas by coating these ZnO bowls with gold by using plasma-induced sputtering and subsequently etching the ZnO with concentrated HCl solution. Figure 5a shows the gold replicas of the bowls. The EDX analysis shows only gold peaks after acid treatment.

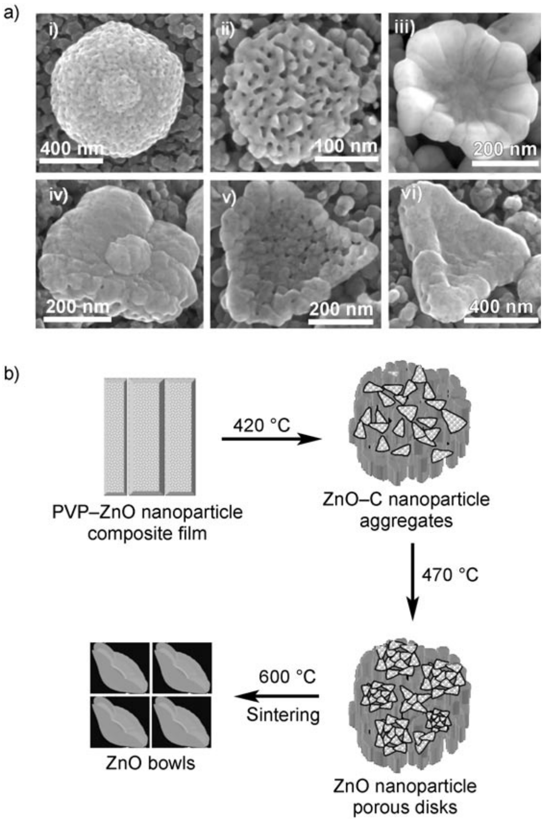

Figure 4. Extraction of intermediate morphologies for different calcination times at 470 °C: a) Emergence of bowl- and troughlike morphologies from the bladelike ZnO–PVP composite. i, iv) Calcination of the composite at 470 °C for 1 h resulted in the formation of circular and triangular composite structures; ii, v) calcination at 470 °C for 5 h resulted in a porous morphology owing to the removal of the polymer; iii, vi) calcination at 470 °C for 8 h transformed these porous structures into zeptoliter bowls and triangular troughs. b) Schematic illustration of the formation of ZnO bowls.

Similarly, silica rings were also made by using ZnO nanorings as the template. The pearl-like silica structures shown in Figure 5b are composed of 12 to 15 nanoparticles of about 50 nm in diameter. In principle, it would be possible to prepare zeptoliter bowls of various metal oxides with this method by optimizing the synthesis conditions. Preliminary experiments with manganese nitrate–PVP also yielded manganese oxide bowls (see the Supporting Information, 7) of diameter 500 nm, but these are less shallow than the ZnO bowls.

Experimental Section

Synthetic procedure for ZnO bowls: In a typical synthesis, $Zn(NO_3)_2{\cdot}6H_2O$ (0.50 g, Merck) was dissolved in ethanol (10 mL) and mixed with poly(vinyl pyrrolidone) (1.00 g, Aldrich, $M_w = 1300000$) to make a homogeneous, viscous slurry. The slurry was then poured into a glass petri dish (50 mm diameter) and aged for 10 h in an oven at 80 °C. The transparent film of zinc nitrate–PVP composite thus obtained was calcined at different temperatures (250, 370, 420, 470, and 600 °C) for a duration of 5 h with a heating rate of 1 °C min^{-1}. Calcinations at 470 °C for different durations (1 h, 5 h, and 8 h) were

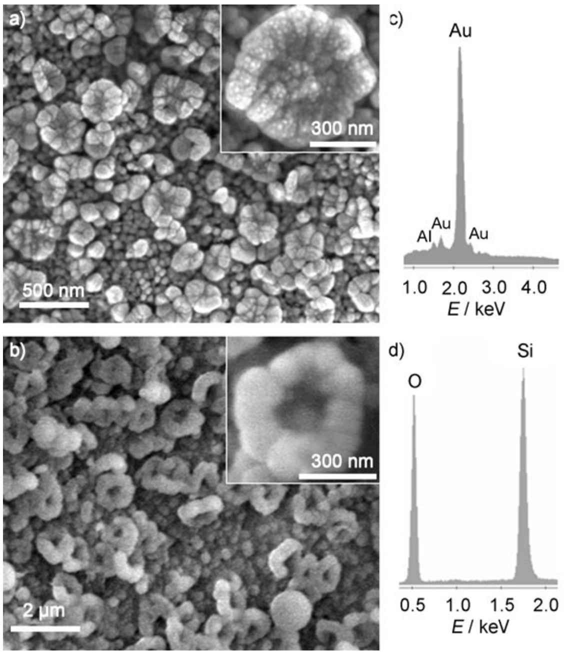

Figure 5. Metal and metal oxide replicas synthesized using ZnO bowls and rings as templates. a) Gold bowls synthesized using ZnO bowls as the template. b) Silica rings templated by ZnO rings. c, d) The corresponding EDX spectra for Au bowls and silica rings after the removal of ZnO. The Al peak arises from the sample holder.

also carried out to understand the bowl formation. In all the cases the sample was cooled to room temperature at a rate of $3\,^{\circ}\mathrm{C\,min^{-1}}$.

Synthetic procedure for gold bowls and silica nanorings using ZnO bowls and nanorings as templates: a) To prepare gold replicas of the ZnO bowls, gold was sputtered onto a sample of ZnO bowls (10 mg) by using a plasma-induced sputtering technique for 2 minutes in an argon atmosphere, which resulted in a coating (ca. 60 nm) of gold over the bowls. The ZnO was removed by soaking the gold-sputtered sample in concentrated HCl solution for 5 min. Finally, the sample was washed thoroughly with deionized water and dried at room temperature.

b) Silica nanorings were obtained by dispersing ZnO nanorings (30 mg) in 2-propanol (3 mL). Deionized water (0.4 mL), ammonia solution (0.1 mL), and tetraethylorthosilicate (TEOS, 0.06 mL) were consecutively added with stirring. The stirring was allowed to continue for 3 h, and a white product was collected after 3 h. The product was filtered and the precipitate was washed several times with deionized water and subsequently anhydrous ethanol. The product (ZnO/SiO_2 core–shell nanorings) was then dried at room temperature. Soaking the product in 6 M HCl solution at room temperature for 3 h removed the ZnO and left the silica rings intact. The solution was filtered and the precipitate was washed several times with deionized water and anhydrous ethanol to obtain silica nanorings.

Sample characterization: The morphologies of the samples obtained in all the experiments were examined with a field-emission scanning electron microscope (FESEM, FEI Nova-Nano SEM-600, The Netherlands) and TEM (JEOL JEM-3010 with an accelerating voltage at 300 kV). Powder X-ray diffraction (XRD) patterns were measured by using a RICH-SIEFERT 3000-TT diffractometer employing $Cu_{K\alpha}$ radiation. Thermogravimetric analysis (TGA) was carried out with a Mettler Toledo TGA 850 instrument. N_2 adsorption–desorption isotherms were measured using a QUANTACHROME AUTOSORB-1C surface-area analyzer at liquid-nitrogen temperature (77 K). AFM images of the nanobowls were acquired in tapping mode on a Digital Instruments CP II AFM (Veeco Instruments Inc., Santa Barbara, CA).

Received: April 21, 2007
Published online: July 2, 2007

Keywords: nanostructures · scanning probe microscopy · self-assembly · zinc oxide

---

[1] S. Mann, G. A. Ozin, *Nature* **1996**, *382*, 313–318.
[2] H. Yang, N. Coombs, G. A. Ozin, *Nature* **1997**, *386*, 692–695.
[3] J. Park, V. Privman, E. Matijevic, *J. Phys. Chem. B* **2001**, *105*, 11630–11635.
[4] M. Li, H. Schnablegger, S. Mann, *Nature* **1999**, *402*, 393–395.
[5] C. Pacholski, A. Karnowski, H. Weller, *Angew. Chem.* **2002**, *114*, 1234–1237; *Angew. Chem. Int. Ed.* **2002**, *41*, 1188–1191.
[6] S. Mann in *Biomineralization: Principles and Concepts in Bioinorganic Materials Chemistry*, Oxford University Press, Oxford, **2001**.
[7] C. Sanchez, H. Arribart, M. G. Guille, *Nat. Mater.* **2005**, *4*, 277–287.
[8] S. Mann, *Angew. Chem.* **2000**, *112*, 3532–3548; *Angew. Chem. Int. Ed.* **2000**, *39*, 3392–3406.
[9] T. Nakajima, H. Nameta, S. Mishima, I. Matsuzaki, K. A. Tanabe, *J. Mater. Chem.* **1994**, *4*, 853–858.
[10] W. J. E. Beek, M. M. Wienk, R. A. J. Janssen, *Adv. Mater.* **2004**, *16*, 1009–1013.
[11] X. Wang, C. J. Summers, Z. L. Wang, *Nano Lett.* **2004**, *4*, 423–426.
[12] M. Huang, S. Mao, H. Feick, H. Yan, Y. Wu, H. Kind, E. Weber, R. Russo, P. Yang, *Science* **2001**, *292*, 1897–1899.
[13] J. Reemts, A. Kittel, *J. Appl. Phys.* **2007**, *101*, 013709.
[14] Z. L. Wang, *J. Phys. Condens. Matter* **2004**, *16*, R829-R858.
[15] J. Y. Lao, J. G. Wen, Z. F. Ren, *Nano Lett.* **2002**, *2*, 1287–1291.
[16] Z. L. Wang, *Mater. Today* **2004**, *7*, 26–33.
[17] Z. W. Pan, Z. R. Dai, Z. L. Wang, *Science* **2001**, *291*, 1947–1949.
[18] W. L. Hughes, Z. L. Wang, *J. Am. Chem. Soc.* **2004**, *126*, 6703–6709.
[19] X. Y. Kong, Z. L. Wang, *Nano Lett.* **2003**, *3*, 1625–1631.
[20] C. X. Xu, X. W. Sun, Z. L. Dong, M. B. Yu, *Appl. Phys. Lett.* **2004**, *85*, 3878–3880.
[21] X. Y. Kong, D. Yong, R. Yang, Z. L Wang, *Science* **2004**, *303*, 1348–1351.
[22] F. Li, Y. Ding, P. Gao, X. Xin, Z. L. Wang, *Angew. Chem.* **2004**, *116*, 5350–5354; *Angew. Chem. Int. Ed.* **2004**, *43*, 5238–5242.
[23] C.-L. Kuo, T. J. Kuo, M. H. Huang, *J. Phys. Chem. B* **2005**, *109*, 20115–20121.
[24] N. S. John, N. R. Selvi, M. Mathur, R. Govindarajan, G. U. Kulkarni, *J. Phys. Chem. B* **2006**, *110*, 22975–22978.
[25] J. E. Barton, T. W. Odom, *Nano lett.* **2004**, *4*, 1525–1528.
[26] Y. Rondelez, G. Tresset, K. V. Tabata, H. Arata, H. Fujita, S. Takeuchi, H. Noji, *Nat. Biotechnol.* **2005**, *23*, 361–365.
[27] S. H. Im, U. Jeong, Y. Xia, *Nat. Mater.* **2005**, *4*, 671–675.